

## Facile preparation for robust and freestanding silk fibroin films in a 1-butyl-3-methyl imidazolium acetate ionic liquid system

Lu Li,<sup>1</sup> Yanna Xiong,<sup>1</sup> Shitao Yu,<sup>1</sup> Shiwei Liu,<sup>1</sup> Fusheng Liu,<sup>1</sup> Congxia Xie<sup>2</sup>

<sup>1</sup>College of Chemical Engineering, Qingdao University of Science and Technology, 53 Zhengzhou Road, Qingdao 266042, People's Republic of China

<sup>2</sup>Key Laboratory of Eco-Chemical Engineering (Ministry of Education), College of Chemistry and Molecular Engineering, Qingdao University of Science and Technology, 53 Zhengzhou Road, Qingdao 266042, People's Republic of China

Correspondence to: L. Li (E-mail: zhanglilu@126.com) or S. Yu (E-mail: yushitaoqust@126.com)

**ABSTRACT:** Silk fibroin film (SFF) with excellent mechanical properties was prepared for the first time with *Bombyx mori* silk fibroin as the material and 1-butyl-3-methyl imidazolium acetate ([Bmim]OAc) ionic liquid (IL) as the solvent. The aim was to understand whether the microstructure of SFF could be modified and whether the mechanical properties were improved when [Bmim]OAc IL was used as a solution. With this new system, the obtained SFF was easily peeled off of the substrate, and the silk fibroin proteins retained the  $\alpha$ -helix secondary structure (silk I). Further test results show that the tensile strength (126.8–129.7 MPa) and anti-UV performance were stronger than the silk fibroin regenerated by traditional ways. Therefore, this study provided and identified a new method with [Bmim]OAc to obtain SFF with strong mechanical properties. This facile preparation and related SFF with excellent mechanical strength could have potential applications in biocompatible implants, synthetic coatings for artificial skin, and many other areas. © 2015 Wiley Periodicals, Inc. *J. Appl. Polym. Sci.* **2015**, *132*, 42822.

**KEYWORDS:** biocompatibility; films; ionic liquids; structure–property relations

Received 26 May 2015; accepted 6 August 2015

DOI: 10.1002/app.42822

### INTRODUCTION

Silk fibroin, produced by the silkworm or *Bombyx mori*, has received extensive interest for its wide use in textiles and consumer products, especially in biomedical materials, for decades. The combination of silk fibroin with medical textiles, such as artificial tendons, blood vessels, and skin grafts, is attractive for the excellent biocompatibility of the protein whether *in vivo* or *in vitro*.<sup>1–10</sup> Among them, the silk fibroin film (SFF), prepared by the drying of the silk fibroin solution, is the one that was studied first and in the most depth. However, the brittleness and poor mechanical properties of SFF limit its applications.<sup>11,12</sup> To improve the mechanical performances, many researchers have adopted blending, grafting, or crosslinking to prepare mixed SFFs.<sup>13</sup> This improved the mechanical properties to some extent, but the introduction of alien species led to nonuniform degradation and to a decrease in the biocompatibility, and this narrowed the application scope. Moreover, harsh conditions, harmful substances residues, environmental pollution, and so on are obstacles during the preparation process. Therefore, it is difficult to prepare a

pure SFF with good mechanical properties with the existing production process.

It is well known that the intrinsic characteristics of the protein molecule are generally regarded as the main reason SFFs are brittle and have poor mechanical properties. From the chemical point of view, silk fiber is a polyamide, one kind of insoluble protein. The length of the C–N bond in the peptide bond (–CO–NH–) of the silk fiber chains was 0.132 nm, which was a little shorter than that of the C–N single bond (0.147 nm) and longer than that of the C=N double bond (0.127 nm), so the peptide bond had some rigidity and flexibility in the macromolecular backbone of the silk protein.<sup>14,15</sup> During the film-formation process, the structure of silk fibroin transformed from a curl into a  $\beta$ -sheet structure, which could form large hydrogen bonds between the side chain and main chain or different side chains and generate the secondary crosslinking between the molecules as well.<sup>12</sup> From the previous analysis, the main factor that affected the mechanical properties of the film was the molecular structure of the fibroin protein. Fortunately, the molecular structure could be adjusted in the dissolution and filming processes;<sup>16</sup> therefore, it will be the key technology for

Additional Supporting Information may be found in the online version of this article

© 2015 Wiley Periodicals, Inc.

the preparation of SFFs with good performances in the selection of the appropriate solvent and SFF-forming process.

Ionic liquids (ILs) are promising alternatives of green solvents for their specific properties, such as the negligible vapor pressure, broad liquid regions, high thermal stabilities, and lack of a burning or explosive point.<sup>17</sup> They have been widely used in the fields of electrochemistry, organic synthesis, separation, and material preparation for their excellent solubility for inorganic compounds, organic compounds, and polymer material.<sup>18</sup> Swatloski *et al.*<sup>19</sup> found that the IL 1-butyl-3-methyl imidazolium chloride ([Bmim]Cl) could be used to obtain solutions of up to 25% w/w cellulose. Then, [Bmim]Cl was used to dissolve silk fibroin, and the temperature was maintained at 100°C. The resulting IL/silk solutions were used to prepare films with methanol or acetonitrile as coagulants. This was the first research on silk films prepared from IL systems, but the films obtained could not be peeled off of the substrate.<sup>6,20</sup> Tsukruk<sup>6</sup> adopted layer-by-layer assembly to prepare robust ultrathin SFFs in a [Bmim]Cl system, but the obtained film was of low elongation within 0.5–3%, which was significantly lower than the elongation of 20–30% routinely achieved for bulk silk materials and oriented fibrils. Furthermore, the filming process was complex and hard to control; this greatly limited the wide application of the technology. On the other hand, with the use of chloride-based IL as the solvent, although the residual electronegativity chloride was small, the biocompatibility of the film was reduced.<sup>21</sup>

The solubility of silk fibroin in ILs depends on the identity of both the cation and anion, where the anion had a much larger effect. The more the cation and anion are able to participate in hydrogen bonding, the better the solubility of the silk fibroin is.<sup>19</sup> According to the previous theory, in this study, the SFFs were prepared via 1-butyl-3-methyl imidazolium acetate ([Bmim]OAc) solvent as the dope in a simple casting process for the first time. The negative ion of acetic acid (OAc<sup>-</sup>) was of better biocompatibility than Cl<sup>-</sup>, and [Bmim]OAc was of lower viscosity than [Bmim]Cl;<sup>22</sup> therefore, the film from the [Bmim]OAc system may have had better properties than that from [Bmim]Cl system. The morphology and mechanical properties of the film were examined. Moreover, the characteristic of the SFF, such as the anti-UV properties, swelling ratio (SR), and porosity ratio, were studied.

## EXPERIMENTAL

### Materials

[Bmim]OAc was synthesized according to a method reported in the literature<sup>23</sup> (see Scheme S1 in the Supporting Information). The other reagents were all purchased from Aldrich and were not purified.

### Preparation of the Silk Film in the [Bmim]OAc IL

The silk was obtained from *B. mori* silkworms (Shandong, China). Live pupae were extracted from the cocoons before sericin removal to prevent contamination of the fibroin protein. Silk fibers were prepared as previously described.<sup>23</sup> Briefly, silkworm cocoons were soaked in a 0.5 wt % Na<sub>2</sub>CO<sub>3</sub> solution, heated, and kept at 90°C for 1 h.<sup>20</sup> The silk fiber was then extensively washed with deionized water and dried overnight *in vacuo*. Extracted silk

fibroin fibers were dissolved in [Bmim]OAc IL (made by our laboratory) to form a 15% w/w solution. The dissolution was completed by the heating of the mixture of the silk fiber and [Bmim]OAc to 65°C for 10 h. The silk/[Bmim]OAc solution was used to cast films on glass slides as the substrate, and the substrate was put aside at 25°C and 65% relative humidity for 1–2 h; then, it was submerged in ethanol as a coagulant, and the IL was extracted out of the silk solution into the ethanol bath. This resulted in the crystallization of the silk fibroin protein into the  $\alpha$ -helix secondary structure.<sup>11,24</sup> After treatment, the SFF was peeled off of the substrate and placed into a deionized H<sub>2</sub>O bath and dried at room temperature.

### Preparation of the Traditional Silk Fibroin Film (TSFF)

The degummed silk was dissolved in 9.3 mol/L LiBr and concentrated to a 15% protein concentration by 10% poly(ethylene glycol). The solution was used to cast films on glass slides as a substrate, and the substrate was put aside at 25°C and 65% relative humidity for 1–2 h. Then, it was submerged in an aqueous 30% w/v ammonium sulfate coagulant solution at 60°C. After treatment, the film was peeled off of the substrate and placed into a deionized H<sub>2</sub>O bath and then dried at room temperature.<sup>23</sup>

### Rheological Experiment on Silk/IL Solvent

A solution (100 mL) containing a certain amount of silk was prepared by the dissolution of the silk in [Bmim]OAc at room temperature. After it was filtered and ultrasonicated to remove trapped air bubbles, the final solution was colorless, and the pH was 7–8. The rheological characterization of the samples was performed in a C-VOR rheometer from Bohlin Instruments, Inc., fitted with a cone-and-plate geometry (cone angle = 4° and diameter = 20 or 40 mm) and a circulating environmental system for temperature control. The rheometer used was a shear-stress-controlled instrument that applied a torque (force) and measured the resulting displacement (movement). Torque and displacement were converted to a rheological format by means of the measurement of the system constants. To prevent the drying of the samples during the experiments, a steel ring with a diameter of 60 mm was placed around the measuring geometry, the annulus was filled with water, and the sample holding region was sealed with an insulated cover. As soon as the sample was introduced into the plate, the data were collected. The test methods used were oscillatory temperature, time, stress, and frequency sweeps at a constant temperature of 25°C and a pH of 7–8.<sup>25</sup>

### Tensile Testing of the Silk Films

The tensile properties were determined by an Instron tensile tester. We tested the tensile strength of the film by fixing it into the two gauges. The test specimen was 20 mm (length of the film > 20 mm) with a pulling speed of 10 mm/min. The average values of the maximum stress and maximum strain were taken after 10 pieces were tested for each measurement. The porosity was obtained from the measurement of dimensions and weight.<sup>26</sup>

### SR of the Films

SR was determined by the immersion of preweighed dry films in buffer solutions (prepared from Na<sub>2</sub>HPO<sub>4</sub> and NaH<sub>2</sub>PO<sub>4</sub>,

pH 7.4) at room temperature. The weight increment of the films was monitored gravimetrically as a function of time. The weights of the samples in the swollen state at different times ( $m_t$ 's) were measured after the gentle removal of excess water with filter paper. The SR was calculated as follows:

$$\text{SR (\%)} = \frac{m_t - m_0}{m_0}$$

where  $m_0$  is the weight of the samples in the dry state.<sup>27</sup>

### Crystalline Structure of the Silk Films

To investigate the crystalline structure of the silk films, wide-angle X-ray scattering (WAXS) experiments were performed in transmission mode with a Rigaku D/max-2500 with monochromatic Cu K $\alpha$  radiation ( $\lambda = 0.1371$  nm), and the scattering vector was calibrated with aluminum oxide. The structure of the films was also analyzed with a Fourier transform infrared (FTIR) spectrometer (Nicolet iN10, Thermo Fisher) attenuated total reflection (ATR) objective to eliminate the effect of water from KBr method, the spectra were collected over the range of 1700–1500  $\text{cm}^{-1}$ .

### Thermal Properties of the Silk Films

The thermal properties of the silk films were measured in a thermogravimetric analysis instrument (Netzsch STA 409PC, Germany) from 50 to 400°C at a heating rate of 10°C/min.

### Average Thickness and Cross-Sectional Area of the Films

We evaluated the average thickness and cross-sectional area with a scanning electron microscope (JSM-6700F field emission scanning electron microscope, JEOL Japan).<sup>28</sup> The morphology and surface roughness of the SFFs were investigated with a Dimension 3000 atomic force microscope (Digital Instruments) in the tapping mode according to procedures adapted in the laboratory.<sup>29</sup>

### Film Stability under UV Light

The film stability against the UV light was studied for silk films from different synthetic methods. The silk film was exposed to a UV light from a 300-W Hg–Xe lamp at a constant temperature (298 K) for 24 h. The variation in the tensile properties of the films were evaluated with an Instron tensile tester.<sup>30</sup>

### Regeneration and Recycling of [Bmim]OAc

After the casting of the film, the solution in the coagulation bath was gathered into a flask and was then distilled. During the distillation, the ethanol was gathered as a fraction, the solution became thicker, and [Bmim]OAc was obtained. At the same time, the distillation was terminated, and the flask was allowed to cool to room temperature. [Bmim]OAc was dried *in vacuo* at 60°C for 24 h; the recovery rate of [Bmim]OAc and ethanol was above 90%.

## RESULTS AND DISCUSSION

### Preparation of the SFF

Silk fibroin is a fibrous protein; however, the microstructure and porosity of regenerated silk-based films and the features involved in cell interactions can be changed by the exploitation of different preparation processes.<sup>31–33</sup> In this study, we adopted a new method for preparing SFFs. A 15% w/w silk fibroin/[Bmim]OAc solution was used to cast the films onto glass slides



**Figure 1.** Regenerated silk film from [Bmim]OAc (SFF). [Color figure can be viewed in the online issue, which is available at [wileyonlinelibrary.com](http://wileyonlinelibrary.com).]

as substrates. Before the substrate was put into coagulant to remove [Bmim]OAc, it was put aside at 25°C and 65% relative humidity for 1–2 h. During this process, the silk fibroin was exposed at the air–solution interface to ensure enough time for the high-molecular-weight fibroin chains to self-assemble. The goal was to generate silk films with a high silk I ( $\alpha$ -helix secondary structure) that more closely mimicked the natural process during silk processing.<sup>2,34,35</sup> Next, the film was easily peeled off of the substrate and then dried at room temperature. Through this method, we obtained a freestanding silk film; the photograph of the film is shown in Figure 1. As shown in Figure 1, the film was colorless, smooth, and transparent. The film obtained was macroscopically smooth and uniform, although as shown in a typical atomic force microscopy (AFM) image [Figure 2(A)], occasional islands were found on the film surface at higher magnifications; this indicated some aggregation of the material in solution before spin casting. The surface micro-roughness was  $20 \pm 3$  nm [Figure 2(B)].

### Structure of SFF as Determined by WAXS and FTIR–ATR Spectroscopy

The structure of the SFF cast from the [Bmim]OAc IL solution under ambient conditions was determined by WAXS and FTIR–ATR spectroscopy. In previous studies, three silk fibroin conformations were identified by WAXS diffraction and IR spectroscopy: random coil,  $\alpha$  form (silk I, type II  $\beta$ -turn), and  $\beta$  form (silk II, antiparallel  $\beta$ -pleated sheet).<sup>2,36</sup> Figure 3(A) shows the WAXS data for the SFF sample, where the SFF exhibited the typical crystal structure. The SFF film showed the typical WAXS diffractogram of the silk I structure, with diffraction peaks at 11.28, 21.52, 22.74, and 27.44°; these corresponded to silk I crystalline spacings of 0.71, 0.43, 0.40, and 0.31 nm, respectively. Furthermore, the peak at spacing near 0.72 nm was strong evidence for the silk I structure.<sup>37,38</sup> No typical diffraction peaks of silk II were found for the SFF. Thus, the silk fibroin in this film was mostly in  $\alpha$ -helix form.

The structure of SFF was also confirmed by FTIR–ATR spectroscopy [Figure 3(B)]. The IR spectral region within 1700–1500  $\text{cm}^{-1}$  was assigned to absorption by the peptide backbones of amide I (1630–1610  $\text{cm}^{-1}$ ) and amide II (1600–1500  $\text{cm}^{-1}$ ), which have been commonly used for the analysis of different secondary structures of silk fibroin.<sup>38–40</sup> In this study, there



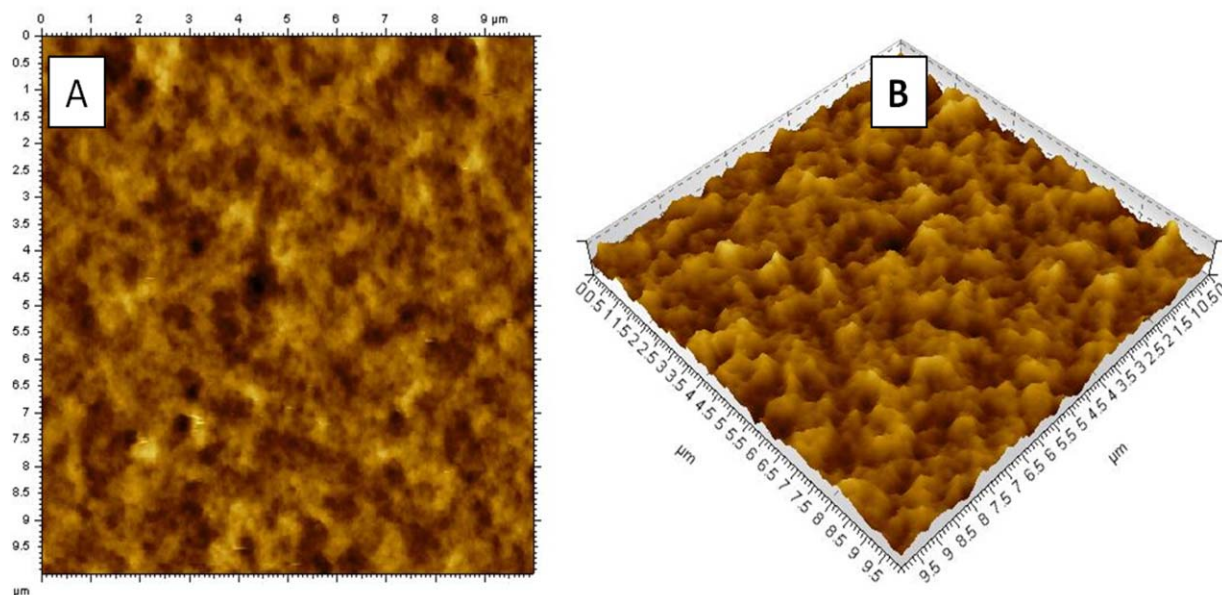


**Figure 2.** AFM image of SFF. [Color figure can be viewed in the online issue, which is available at [wileyonlinelibrary.com](http://wileyonlinelibrary.com).]

were two obvious peaks in Figure 3(B). One peak was at  $1630\text{ cm}^{-1}$ , and this corresponded to the amide I band. The other peak was at  $1574\text{ cm}^{-1}$  and corresponded to amide II; it was stronger than the peak at  $1630\text{ cm}^{-1}$ . The FTIR results show that the film mainly had an  $\alpha$ -helix secondary structure; this was consistent with the WAXS results and confirmed that the main secondary structure of SFF was an  $\alpha$ -helix.

#### Thermogram of the SFF

The thermogram of the SFF (Figure 4) showed two endothermic peaks only, one at about  $96^\circ\text{C}$  and one at about  $279.2^\circ\text{C}$ ; these corresponded, respectively, to H-bonded water molecule departure and silk melting–decomposition.<sup>35,41</sup> There was no

exothermic peak, and this implied that silk I was a stable crystal, which never transformed into a  $\beta$  sheet above the glass-transition temperature.<sup>38</sup> In conclusion, the thermogram clearly evidenced that the SFF had a stable silk I crystal structure; this was in agreement with WAXS and FTIR spectroscopy.

#### Rheology of a Silk Fibroin/IL Solution

We also used a novel method to prepare a freestanding silk film from 15% w/w silk fibroin/[Bmim]Cl solution, but the film obtained was difficult to peel off of the substrate. It can be supposed that the nature of anions in the [Bmim] IL may have considerably influenced the physicochemical properties of the silk fibroin/IL solutions. Therefore, we studied the rheology of

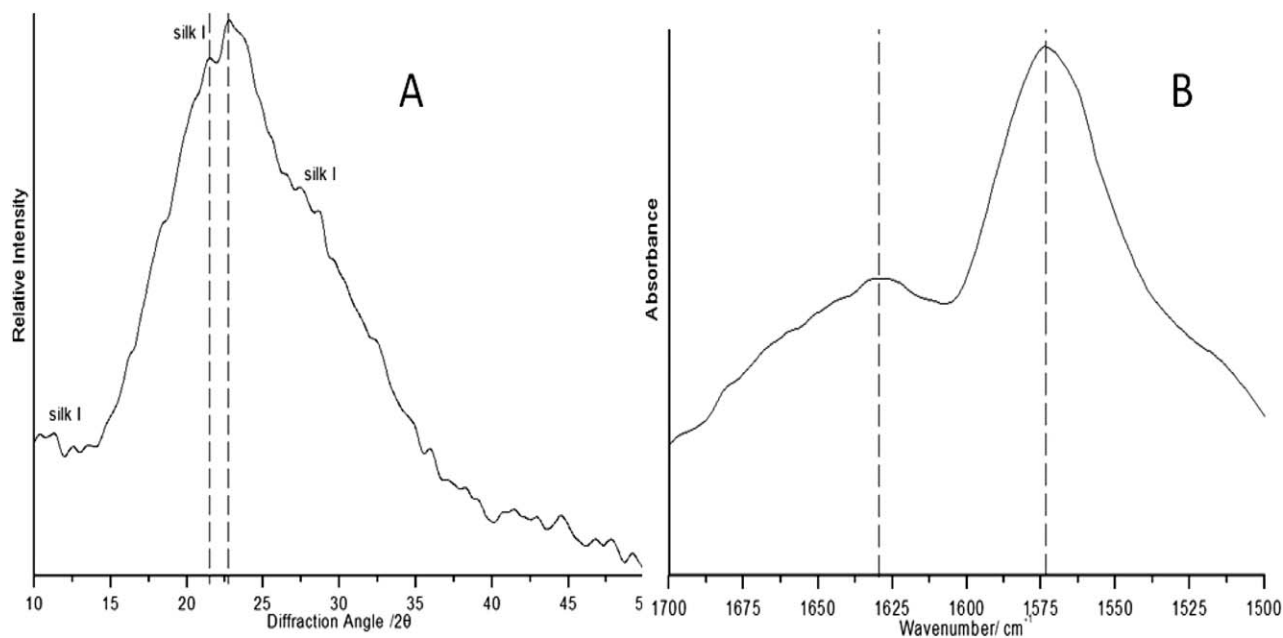


**Figure 3.** (A) WAXS and (B) FTIR–ATR spectra of SFF cast from an IL solution under ambient conditions.

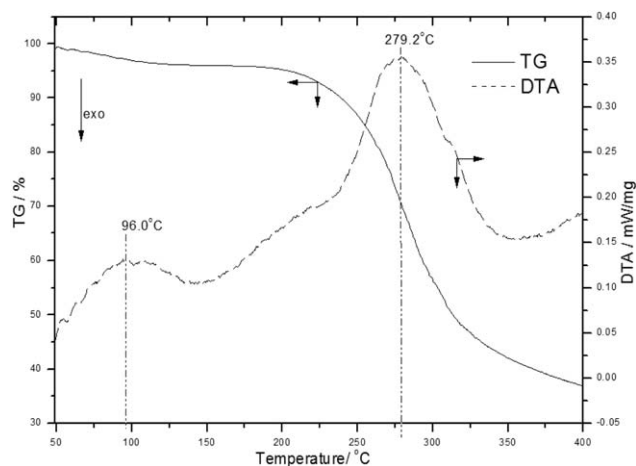


**Figure 4.** Thermogravimetry (TG) and differential thermal analysis (DTA) curves for SFF.

the silk fibroin solutions in two ILs composed of the [Bmim] cation and different anions: chloride and acetate. With the temperature and viscosity values of the 15% w/w silk fibroin/[Bmim]Cl solution and 15% (W/W) silk fibroin/[Bmim]OAc solution taken as coordinates, the flow activation energy ( $E_{\eta}$ ) was calculated by the slope of the line obtained (Figure 5). As a result, the  $E_{\eta}$  of the 15% w/w silk fibroin/[Bmim]Cl solution reached 123.4 kJ/mol, whereas that of the 15% w/w silk fibroin/[Bmim]OAc solution was only 41.5 kJ/mol. It is well known that  $E_{\eta}$  indicates that the molecular chain is a minimum energy to overcome the barrier moving from the original position to near the hole, and it is relative to the structure of the molecular chain and not relative to the molecular weight. In general, the more rigid, the stronger the polarity, or the larger the side groups of the molecular chain, the higher  $E_{\eta}$  will be.<sup>42</sup> This suggests that the degree of tangling of silk fibroin molecular chains was lower in the [Bmim]OAc solution than in the [Bmim]Cl solution, so the molecular chain only needed to overcome the low  $E_{\eta}$  to realize movement in the [Bmim]OAc solution; this was advantageous to the arrangement of the molecular chain. When the SFF was prepared through the [Bmim]OAc solution, the molecular chain was arranged along the same direction, and a uniform texture and high strength in the SFF was easily obtained. In addition to the force of the hydrogen bonds, van der Waal's forces between the silk fibroin molecules formed a physical crosslinking point, and these crosslinking points in the silk fibroin/IL solution were in dynamic equilibrium between constant segregation and recombination, so the system of the silk fibroin/IL solution formed an instantaneous imitate network structure.<sup>25</sup> In the low shearing rate regions, the tangling points and apparent viscosity remained unchanged; this indicated that the two systems were first in the Newtonian region (Figure 6).<sup>43</sup> When the shear rate increased to a certain extent, part of the tangling points in the [Bmim]Cl solution divided and could not regroup quickly, so the apparent viscosity decreased, and the flow behavior exhibited shear thinning. On the contrary, for the [Bmim]OAc solution, most of the divided tangling points could be rebuilt in a timely manner, despite the fact that the apparent viscosity also decreased, but the rate of

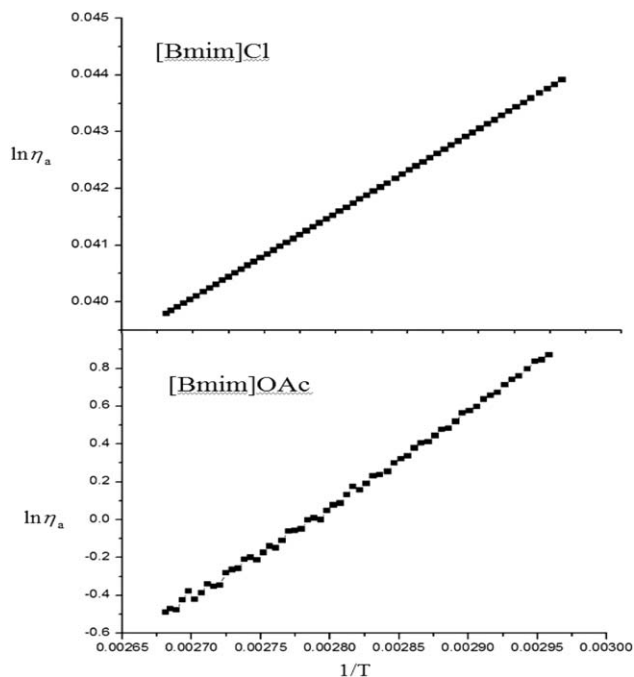


**Figure 5.** Curves of the  $\ln \eta_a \sim 1/T$  slope for silk fibroin/[Bmim]OAc and silk fibroin/[Bmim]Cl ( $\eta_a$ , kJ/mol;  $T$ , K), where  $\eta_a$  is the flow activation energy,  $T$  is temperature.

decline was very small; this was relative to the low  $E_{\eta}$  and the flexible molecular chain. In a word, the silk fibroin/[Bmim]OAc solution had a low  $E_{\eta}$  and a relatively stable apparent viscosity; it was advantageous that the silk fibroin molecular chain overcame the barrier and supplied the defects in a timely manner to

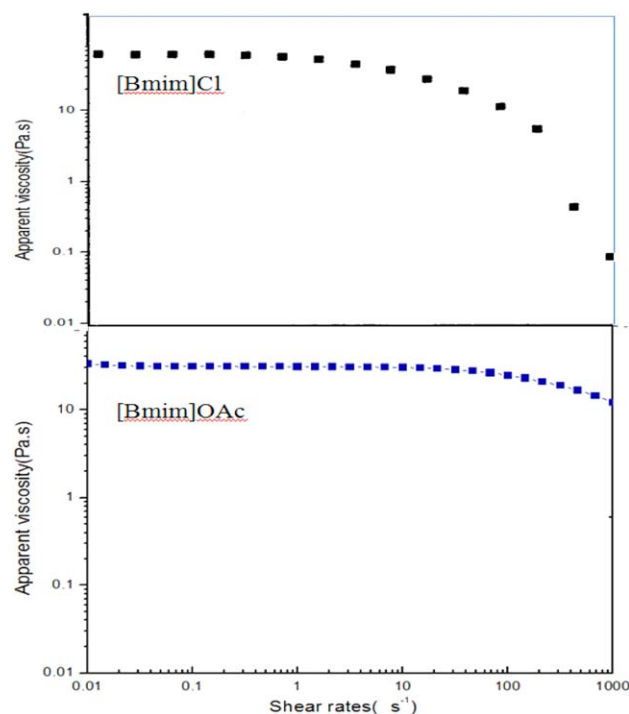


**Figure 6.** Apparent viscosity of 15% silk fibroin/[Bmim]OAc and 15% silk fibroin/[Bmim]Cl. [Color figure can be viewed in the online issue, which is available at [wileyonlinelibrary.com](http://wileyonlinelibrary.com).]

**Table I.** Mechanical Properties of SFFs with Different Fabrication Processes

Film <sup>a</sup>	SEM thickness ( $\mu\text{m}$ ) <sup>b</sup>	AFM roughness (nm) <sup>c</sup>	Tensile strength (MPa)	Elongation at break (%)	SR (%)	Porosity (%)	Tensile strength (MPa) <sup>d</sup>
SFF	4.63	20 $\pm$ 3	128.3 $\pm$ 1.5	17.5 $\pm$ 2.2	36.8 $\pm$ 1.5	55.6 $\pm$ 0.5	120.8 $\pm$ 1.5
TSFF	5.97	22 $\pm$ 5	65.0 $\pm$ 1.3	20 $\pm$ 2.0	25.9 $\pm$ 1.2	19.1 $\pm$ 0.6	31.3 $\pm$ 1.3

<sup>a</sup>All of the films were dried under identical conditions after treatment.

<sup>b</sup>For SEM of SFF and TSFF, see Figure S2 in the Supporting Information.

<sup>c</sup>For AFM of TSFF, see Figure S3 in the Supporting Information.

<sup>d</sup>Treated with UV.

the process of filming. Therefore, a pure freestanding SFF was easily obtained with [Bmim]OAc as the solvent.

### Mechanical Properties of SFF

We also studied the mechanical properties of SFF and compared them with TSFF; the related results are shown in Table I. As shown in Table I, the tensile strength of SFF was 126.8 MPa; this was greater than that of TSFF (62.4 MPa), and the elongation of SFF was slightly lower than that of TSFF. This could be explained as follows. To remove the low-molecular-weight components present in the original degummed silk, TSFF was prepared by reverse dialysis against poly(ethylene glycol) in our process for concentrating silk fibroin, whereas fibroin fragments, larger than approximate 12 kDa and produced by chain scission in the LiBr during dissolution, were retained.<sup>44</sup> Of course, poly(ethylene glycol) could not be transferred to the solution during reverse dialysis and could not contribute to the mechanical properties of TSFF. However, for the large fibroin fragments in the LiBr solution, fibroin molecules aggregated and caused orientation asymmetry. This hypothesis was confirmed by the image on the cross section of film from scanning electron microscopy (SEM; Figure S1). As shown in Figure S1 (see the Supporting Information), the cross section of SFF (Figure S1B) was smooth and uniform, but the cross section of TSFF was rough, uneven, and inadequate (Figure S1A). It is a general truth that the orientation and crystallinity of fibroin molecules affects the intensity of films. With increasing degree of orientation, the degree of order and crystallinity were enhanced. Furthermore, the strength of the film was amplified, and the elongation was lessened. It is worth noting that the porosity of the SFF was 55.3%, but that of TSFF was only 18.9% (Table I). This difference was also caused by the fibroin molecule aggregation and orientation in different preparation systems. In the [Bmim]OAc system, the silk fibroin dissolved completely, so the fibroin molecular uniformly dispersed. When SFF regenerated, the fibroin molecules were rearranged by the stable antiparallel  $\beta$ -sheet structure, so the shapely pore formed.<sup>24</sup> On the

contrary, in the LiBr system, there was a much larger fibroin molecular aggregate, and this led to an unordered molecular orientation during the formation of TSFF. Therefore, the porosity of TSFF was low, and as a result, the SR of TSFF was also lower than that of SFF (Table I). Interesting, from 126.8 to 120.2 MPa, the tensile strength of SFF decreased about 5.2% after UV treatment for 24 h, but for the TSFF, the tensile strength decreased up to 51.4% from 62.4 to 30.3 MPa (Table I). This proved that the SFF made by the new method could be more resistant to UV than the routine method. This could be better explained by the silk fibroin molecular alignment. In SFF, it was more loose and orderly than in TSFF. Therefore, when UV was irradiated on the two different films, the good orderly molecular alignment of SFF could refract some section of UV to slow the intensity change of UV, and at the same time, the tensile strength of SFF slightly decreased when compared with TSFF. In brief, [Bmim]OAc was an excellent solvent for the silk fibroin to prepare films with outstanding mechanical properties, and this new simple method would promote the deep development of SFFs through various aspects.

### Regeneration of [Bmim]OAc

The regenerated [Bmim]OAc was used as a solution to dissolve silk fibroin to prepare the films. The properties of SFFs prepared with the recycled [Bmim]OAc are shown in Table II. As shown in Table II, the SFFs also had good properties when [Bmim]OAc was used for the second time. This suggested that [Bmim]OAc had excellent stability and could be recycled. Furthermore, this new simple method for preparing SFFs involved only three materials: [Bmim]OAc, ethanol, and silk fibroin. Among them, [Bmim]OAc and ethanol were both recovered by distillation and showed almost no loss, especially for [Bmim]OAc. Therefore, the results of the mechanical properties of SFFs from the regeneration of [Bmim]OAc indicated that the new method for the preparation of SFF was an environmentally friendly and cheap process.

**Table II.** Mechanical Properties of SFF from the Regeneration of [Bmim]OAc as the Solution

Number	SEM thickness ( $\mu\text{m}$ )	AFM roughness (nm)	Tensile strength (MPa)	Elongation at break (%)	SR (%)	Porosity (%)
1	4.63	20 $\pm$ 3	128.3 $\pm$ 1.2	17.5 $\pm$ 2.5	36.8 $\pm$ 0.4	55.6 $\pm$ 0.3
2	4.62	21 $\pm$ 2	126.5 $\pm$ 1.3	16 $\pm$ 2.0	36.0 $\pm$ 0.35	55.0 $\pm$ 0.2
3	4.59	21 $\pm$ 3	124.6 $\pm$ 1.2	17 $\pm$ 2.0	36.6 $\pm$ 0.4	55.3 $\pm$ 0.4

## CONCLUSIONS

In this report, we described and evaluated a novel and environmentally friendly process of the integral film formation of silk fibroin that overcame the limitations of previous process. The SFF obtained had a uniform and smooth cross section and crystal structure close to an  $\alpha$ -helix secondary structure. It is important to emphasize that the SFF obtained with [Bmim]OAc as a solution had better mechanical properties, especially freestanding, than those found in previous studies. The improved mechanical and freestanding properties of the SFF prepared in this study contributed to its use in biomedical applications, such as hernioplasty, skin, or wrinkle filling. Moreover, cheap waste silk as a feedstock and the recycling of [Bmim]OAc and ethanol made it economic. Importantly, our film-formation process can be carried out under clean, sterile, and carefully regulated conditions.

## ACKNOWLEDGMENTS

This work was financially supported by the National Natural Science Foundation of China (contract grant number 21376130) and the Specialized Research Fund for the Doctoral Program of Higher Education (contract grant number 20133719110001).

## REFERENCES

1. Shao, Z.; Vollrath, F. *Nature* **2002**, *418*, 741.
2. Jin, H. J.; Kaplan, D. L. *Nature* **2003**, *424*, 1057.
3. Vollrath, F.; Madsen, B.; Shao, Z. *Proc. R. Soc. Lond. B* **2001**, *268*, 2339.
4. Chen, X.; Shao, Z.; Vollrath, F. *Soft Matter* **2006**, *2*, 448.
5. Lewis, R. V. *Chem. Rev.* **2006**, *106*, 3762.
6. Jiang, C. Y.; Wang, X. Y.; Gunawidjaja, R.; Lin, Y. H.; Gupta, M. K.; Kaplan, D. L.; Naik, R. R.; Tsukruk, V. V. *Adv. Funct. Mater.* **2007**, *17*, 2229.
7. Ohgo, K.; Zhao, C.; Kobayashi, M.; Asakura, T. *Polymer* **2003**, *44*, 841.
8. Brenckle, M. A.; Tao, H.; Kim, S. H.; Paquette, M.; Kaplan, D. L.; Omenetto, F. G. *Adv. Mater.* **2013**, *25*, 2409.
9. Zhou, L.; Chen, X.; Dai, W.; Shao, Z. *Biopolymers* **2006**, *82*, 144.
10. Altman, G. H.; Diaz, F.; Jakuba, C.; Calabro, T.; Horan, R. L.; Chen, J. *Biomaterials* **2003**, *24*, 401.
11. Gupta, M. K.; Khokhar, S. K.; Phillips, D. M.; Sowards, L. A.; Drummy, L. F.; Kadakia, M. P.; Naik, R. R. *Langmuir* **2007**, *23*, 1315.
12. Wongpanit, P.; Tabata, Y.; Rujiravanit, R. *Macromol. Biosci.* **2007**, *7*, 1258.
13. Asakura, T.; Watanabe, Y.; Itoh, T. *Macromolecules* **1984**, *17*, 2421.
14. Bian, R. Q.; Xiong, J.; Lei, B.; Fan, X.; Xie, J. *Sci. Pap. Online* **2011**, *8*, 1.
15. Li, Z. H.; Ji, S. C.; Wang, Y. Z.; Shen, X. C.; Liang, H. *Front. Mater. Sci.* **2013**, *7*, 237.
16. Heslot, H. *Biochimie* **1998**, *80*, 19.
17. Yue, C. B.; Fang, D.; Liu, L.; Yi, T. F. *J. Mol. Liq.* **2011**, *163*, 99.
18. Zhang, S.; Xu, C. M.; Lu, X. M.; Zhou, Q. *Ionic Liquids and Green Chemistry*; Press of Science: China, **2009**.
19. Swatloski, R. P.; Spear, S. K.; Holbrey, J. D.; Rogers, R. D. *J. Am. Chem. Soc.* **2002**, *124*, 4974.
20. David, M. P.; Lawrence, F. D.; Rajesh, R. N.; Hugh, C. D.; Douglas, M. F.; Paul, C. T.; Robert, A. M. *J. Mater. Chem.* **2005**, *15*, 4206.
21. Engel, P.; Mladenov, R.; Wulfhorst, H.; Jager, G.; Spiess, A. C. *Green Chem.* **2010**, *12*, 1959.
22. Datta, S.; Holmes, B.; Park, J. I.; Chen, Z. *Green Chem.* **2010**, *12*, 338.
23. Lawrence, B. D.; Cronin-Golomb, M.; Georgakoudi, I.; Kaplan, D. L.; Omenetto, F. G. *Biomacromolecules* **2008**, *9*, 1214.
24. Phillips, D. M.; Drummy, L. F.; Conrady, D. G.; Fox, D. M.; Naik, R. R.; Stone, M. O.; Trulove, P. C.; De Long, H. C.; Mantz, R. A. *J. Am. Chem. Soc.* **2004**, *126*, 14350.
25. Li, L.; Yuan, B.; Liu, S. W.; Yu, S. T.; Xie, C. X.; Liu, F. S. *J. Mater. Chem.* **2012**, *22*, 8585.
26. Mallika, P.; Himabindu, A.; Shailaja, D. *J. Appl. Polym. Sci.* **2006**, *101*, 63.
27. Zhao, W. F.; Glavas, L.; Odelius, K.; Edlund, U.; Albertsson, A. C. *Polymer* **2014**, *55*, 2967.
28. Jin, H. J.; Park, J.; Valluzzi, R.; Cebe, P.; Kaplan, D. L. *Biomacromolecules* **2004**, *5*, 711.
29. Tsukruk, V. V.; Bliznyuk, V. N. *Langmuir* **1998**, *14*, 446.
30. Kamada, K.; Tsukahara, S.; Soh, N. *J. Phys. Chem. C* **2011**, *115*, 13232.
31. Jin, H. J.; Fridrikh, S. V.; Rutledge, G. C.; Kaplan, D. L. *Biomacromolecules* **2002**, *3*, 1233.
32. Lu, Q.; Hu, K.; Feng, Q. L.; Cui, F. Z. *J. Biomed. Mater. Res. A* **2008**, *84*, 198.
33. Lu, Q.; Zhang, S. J.; Hu, K.; Feng, Q. L.; Cao, C. B.; Cui, F. Z. *Biomaterials* **2007**, *28*, 2306.
34. Wang, L.; Xie, H.; Qiao, X.; Goffin, A.; Hodgkinson, T.; Yuan, X.; Sun, K. *Langmuir* **2012**, *28*, 459.
35. Sohn, S. K.; Strey, H. H.; Gido, S. P. *Biomacromolecules* **2004**, *5*, 751.
36. Demura, M.; Asakura, T.; Kuroo, T. *Biosensors* **1989**, *4*, 361.
37. Anderson, J. P. *Biopolymers* **1998**, *45*, 307.
38. Lu, Q.; Hua, X.; Wang, X.; Kluge, J. A.; Lu, S.; Cebe, P.; Kaplan, D. L. *Acta Biomater.* **2010**, *6*, 1380.
39. Jin, H. J.; Park, J.; Karageorgiou, V.; Kim, U. J.; Valluzzi, R.; Cebe, P. *Adv. Funct. Mater.* **2005**, *15*, 1241.
40. Wilson, D.; Valluzzi, R.; Kaplan, D. *Biophys. J.* **2000**, *78*, 2690.
41. Aline, P.; Philippe, C.; Céline, P.; Hung, M. D.; Marine, W.; Bernard, M. *Vibr. Spectrosc.* **2014**, *73*, 79.
42. Motoaki, M.; Kosuke, O.; Yuichi, M. *Polymer* **2008**, *49*, 952.
43. Um, C.; Kweon, H. Y.; Park, Y. H.; Hudson, S. *Int. J. Biol. Macromol.* **2001**, *29*, 91.
44. Zhou, G.; Shao, Z.; Knight, D.; Yan, J.; Chen, X. *Adv. Mater.* **2009**, *21*, 366.